Mapping of perovskite oxides in the localized vs itinerant electron diagram and its relation with the ionic conductivity

Sachi Taniguchi, Masaru Aniya*

Department of Physics, Graduate School of Science and Technology, Kumamoto University, Kumamoto 860-8555, Japan

Abstract

The electronic properties of perovskite-type oxides ABO_3 can be characterized by the degree of localization of d-electrons. On the other hand, the complex perovskite oxides $A_{1-x}A'_xB_{1-y}B'_yO_{3-\delta}$ exhibit ionic conduction through the defects created by partial substitution of metal atom A and (or) B. In the present study, the relationship between the ionic conduction and the nature of electronic transport properties in perovskite-type oxides is discussed by extending the classification scheme of localized and itinerant d-electron diagram used for ABO_3 compounds. The classification scheme is based on the potential parameter Z/r, where Z and r are the valence and ionic radii of the cation. From the analysis, it is found that in perovskite oxides, the oxygen ionic conductivity decreases with

Z_A / r_A of ion A. The result indicates that the nature of the electronic state influences the ionic conduction. An interpretation of the result found in terms of the bond fluctuation model of superionic conductors is given.

Keywords: Perovskite oxides, localized and itinerant electrons, ionic conductors

1. Introduction

Mixed oxides with the perovskite structure allow the synthesis of solid solutions containing various ions. They are also promising materials which can combine the properties of electronics and solid electrolytes. Therefore, the search of alternative cathode materials of the complex perovskite-type oxides is attracting much interest in the field of functional ceramics and other fields of applications [1-5]. For the development of functional materials, many investigations concerning the effects of temperature, chemical composition, structure and pressure have been performed to clarify the ionic conduction mechanism and the structural stability. Nevertheless, despite many studies, its understanding from the fundamental point of view remains still unclear. For instance, it is known that the perovskite-type oxides behave as metallic, semiconductive or insulators, depending on the degree of the overlap between the cation and anion orbitals [6]. However, it is not clear how these properties are reflected in the ion transport properties.

Concerning the electronic properties, the d-electrons in transition metal oxides ABO_3 are described as localized or itinerant electrons. A scheme to classify the ABO_3 type perovskite materials as having localized or itinerant d-electrons has been proposed by using Z_A / r_A and Z_B / r_B as ordinate and abscissa, respectively [7]. Here, Z_A and Z_B are the valences of the cations A and B, and r_A and r_B are their ionic radii. On the other hand, it is known that the complex perovskite oxides $A_{1-x}A'_xB_{1-y}B'_yO_{3-\delta}$ exhibit ionic conduction through the defects created by partial substitution of metal atom A and (or) B. Recent studies have revealed that in addition to defects, the nature of the chemical bonding between

cation and anion plays an important role in the ion transport processes [8]. Therefore, clarifying the role of the d-electrons of perovskite materials in the ion transport property is of primordial importance to understand the mechanism of ion conduction in this type of materials. In view of these points, it will be interesting to extend the classification scheme for ABO_3 compounds mentioned above in such a way to include the $A_{1-x}A'_xB_{1-y}B'_yO_{3-\delta}$ oxides, and see how the classification is related with the ion transport properties.

2. Mapping of perovskite oxides

In Fig. 1, the ABO_3 and $A_{1-x}A'_xB_{1-y}B'_yO_{3-\delta}$ compounds are classified in a map proposed by Kamata and Nakamura [7]. The meanings of Z_A / r_A and Z_B / r_B have been mentioned in the Introduction. The dotted line in the figure indicates the boundary between the localized and itinerant d-electron systems. This separation line is based on the classification of ABO_3 compounds [7]. Briefly, in the perovskite structure, B atom is surrounded octahedrally by oxygen atoms. The B-O bonds are essentially covalent due to the participation of d-electrons. An octahedron connects to an adjacent octahedron through the formation of B-O-B bond. If this kind of bond percolates, the electronic transport property will show an itinerant behavior. The electron attracting power of B cation increases with the increase of Z_B / r_B, because it gives a measure of Coulomb interaction. Since the d-electrons orbital has a localized nature, with the increase of Z_B / r_B, the degree of electron localization increases. This explains the trends along the Z_B / r_B axis observed in

Fig. 1. The trend along the Z_A / r_A axis can be understood in the same way, however, without considering the effect of d-electrons. The combined effects of Z_A / r_A and Z_B / r_B determine the localized-itinerant nature of electronic transport shown in the figure.

In Fig. 1, for the complex oxides $A_{1-x}A'_xB_{1-y}B'_yO_{3-\delta}$, (A, A' = La, Ce, Pr, Sr / B, B' = Fe, Co, Ni, Mn), the composition weighted (*x*- and *y*-) average values of Z and r are used. In the determination of Z_B, the charge neutrality condition was also taken into account. Such charge balance is necessary to account for the oxygen defects expressed by δ. For instance, for the case of $Sr_{0.9}Ce_{0.1}FeO_{3-\delta}$ ($\delta = 0.315$), the effective, or composition weighted average valence of the A cation is $Z_A = 0.9\times 2_{(Sr)} + 0.1\times 3_{(Ce)} = 2.1$. By adopting the valence $Z_O = -2$ for the oxygen, the effective valence of B cation is determined from $Z_A + Z_B + (3-0.315)(-2)_{(O)} = 0$, giving $Z_B = 3.27$. That is, the transition metal located at the B site in the perovskite structure can take account for the charge balance by changing the valence. Concerning the ionic radii, the values reported by Shannon were used [9]. The newly added $A_{1-x}A'_xBO_{3-\delta}$, and $A_{1-x}A'_xB_{1-y}B'_yO_{3-\delta}$ compounds shown in Fig. 1 are listed in Table 1. The ABO_3 compounds are those reported in [7]. It is interesting to note from Fig. 1 that complex perovskite oxides are mapped in the itinerant electrons side. However, this observation should be taken carefully, because the demarcation line is not strict as has been noted in a recent study [10]. The important point is to note the gross trend observed in Fig. 1.

3. Relationship between the potential parameters of the cations and the ionic conductivity

Fig. 2 shows the relationship between the oxygen ionic conductivity at T = 1073 K [11] and the potential parameters Z_A / r_A and Z_B / r_B of the cations in complex perovskite oxides. From the figure, we recognize a certain trend. The ionic conductivity decreases with the increase of Z_A / r_A. On the other hand, no clear trend is observed with the values of Z_B / r_B. This suggests that the A cation is playing the role of modulator in the ionic conduction. This observation can be understood as follows. It has been shown recently that the ionicity of A-O bond is larger than that of B-O bond [12]. In other words, the covalency which is caused by the overlap of orbitals is larger in the B-O bond than in the A-O bond. The result is expected due to the presence of d-electrons in B atom, and is consistent with the short bond length of B-O than that of A-O. This implies that the bonding of B-O is strong compared to that of A-O bond. The results of Raman and IR measurements support these conjectures [13]. When there is a large difference in ionicity between A-O and B-O bonds, the oxygen ion will locate near the B site, because the bonding is strong. In contrast, when the difference in ionicity is small, their nature of the chemical bond become closer, and the oxygen ion might bind to B-site or to A-site ions. That is, the site where the oxygen ion is located becomes unstable. This effect will result in the increase of the oxygen ion conductivity. For instance, if we consider the compounds in the line $Z_B / r_B = \text{const}$, the difference of the ionicity between A-O and B-O bonds is written as $\Delta f_i = \left| f_i^{AO} - f_i^{BO} \right| = \left| f_i^{AO} - \text{const} \right|$. That is, the increase of Δf_i or f_i^{AO} or Z_A / r_A (the

Coulomb interaction is proportional to ionicity), will result in the decrease of the ionic conductivity. This is the gross behavior observed in Fig. 2. Here, we have discussed about the role of A cation in the ionic conduction. The role of B cation will be discussed later.

The ionicity f_i^{μ} of the individual bond $\mu = \mathrm{AO}$ or BO mentioned above has been calculated through the extended version of the dielectric theory of electronegativity widely used in the study of multicomponent systems [14, 15]. The chemical bonding of a multicomponent material can be decomposed into binary components A_mO_n or B_mO_n. The fractions of the ionicity f_i^{μ} and covalency f_c^{μ} of any individual bond μ in a multibond crystal are written as,

$$f_i^{\mu} = \frac{(C^{\mu})^2}{(E_g^{\mu})^2}, \qquad f_c^{\mu} = \frac{(E_h^{\mu})^2}{(E_g^{\mu})^2}, \tag{1}$$

where E_g^{μ} is the average energy gap that consists of homopolar E_h^{μ} and heteropolar C^{μ} parts.

$$(E_g^{\mu})^2 = (E_h^{\mu})^2 + (C^{\mu})^2, \tag{2}$$

where

$$E_h^{\mu} = \frac{39.74}{(d^{\mu})^{2.48}} \ \text{(eV)}, \tag{3}$$

$$C^{\mu} = 14.4 b^{\mu} \exp\left(-k_s^{\mu} r_0^{\mu}\right)\left[Z_{\mathrm{A,B}} - \frac{n}{m} Z_{\mathrm{O}}\right]\frac{1}{r_0^{\mu}}, \tag{4}$$

$$b^{\mu} = b(N_c^{\mu})^2, \tag{5}$$

where r_0^{μ} is the average radius, which is a half of the bond length d^{μ}, $\exp(-k_s^{\mu} r_0^{\mu})$ is the Thomas-Fermi screening factor, $Z_{\mathrm{A,B,O}}$ are the number of valence electrons of the atoms A, B and O involved in the formation of bond μ. b^{μ} is a correction factor that is proportional

to the square of the average coordination number N_c^{μ}. In the above equations, d^{μ} and r_0^{μ} are expressed in Å and energy is given in eV.

The relation between Δf_i calculated based on the above expressions and some physical quantities of perovskite materials has been studied [12, 16]. For instance, it has been found that the thermal expansion coefficient decreases with the increase of Δf_i. Based on such a result, an explanation to the empirical correlation reported for O ion conductivity and thermal expansion [11] has been given.

Many studies have stressed the importance of the tolerance factor (*t*-factor) in the ion transport properties of perovskites [17]. The *t*-factor is defined as

$$t = \frac{(r_A + r_O)}{\sqrt{2}(r_B + r_O)} \quad , \tag{6}$$

where r_A, r_B and r_O are the ionic radii of A cation, B cation and oxygen, respectively. The *t*-factor gives a measure of how the crystal structure of a compound deviates from the ideal perovskite structure, $t = 1$.

Fig. 3 shows the relationship between the difference of ionicity and the *t*-factor in $A_{1-x}A'_xB_{1-y}B'_yO$ (A, A' = La, Ce, Pr, Sr / B, B' = Fe, Co, Mg, Ga), For the values of *t*-factor, we have adopted the values reported in [18]. From the figure, we note a correlation between the behaviors of *t*-factor and Δf_i. We note also that with the decrease of the difference in ionicity, the *t*-factor approaches to $t = 1$.

It has been suggested by some authors that good ionic conductors have *t*-factor at around 0.96 [17]. In the light of Fig. 3, this observation suggests that good ionic conductors should

have small value of Δf_i. The result shown in Fig. 4 confirms that the conjecture is true. We can see clearly that the ionic conductivity increases with the decrease of Δf_i. It is also consistent with the discussion given in relation to Fig. 2. That is, the ionic conductivity increases with the decrease of Z_A / r_A.

4. Interpretation in terms of the bond fluctuation model

In previous sections we have seen how the ionic conductivity depends on the potential parameters Z_A / r_A, Z_B / r_B, and on the difference of ionicity. From the analysis, an important concept to understand the origin of ion transport in perovskite materials was gained. In this section, the results obtained are discussed in terms of the bond fluctuation model of superionic conductors [8, 19]. According to the bond fluctuation model, the superionic behavior is related to a change of bonding that occurs locally and fluctuates in time. Since the site where change of bonding occurs is unstable, its propagation triggers new bond fluctuating sites, which result in the correlated ion motions. This kind of ion dynamics has been firmly confirmed by ab initio molecular dynamics studies performed in some Cu and Ag halides and chalcogenides [20]. Experimental studies of temperature dependence of dynamical effective charge also support the existence of bond fluctuation processes [21]. An important message that we can learn from the model is that the fast ion movement occurs in sites where different type of bond coexists [8].

An interesting point that should be noted in Fig. 1 and 2 is that the complex perovskite oxides exhibiting high ionic conduction are located near the demarcation line separating localized and itinerant electrons. This fact has been also noted by another group [22]. This observation is providing a hint to understand the role of electron orbital overlap in the ion transport. As discussed in previous section, the itinerant nature of electron transport changes to a localized nature when the percolation of -B-O-B- covalent bond mediated by d-electrons of B cation is disrupted. According to the bond fluctuation model, such disruption can be triggered by atomic vibration, because the d-electron orbital has a localized nature and its wave function does not spread over long distances. That is, in the light of the bond fluctuation model, the locations of the data points near the localized-itinerant demarcation line can be understood straightly.

5. Conclusion

The classification of the materials in terms of localized and itinerant d-electrons scheme used for ABO_3 compounds was extended to complex perovskite oxides. Based on the classification, the relationship between the ionic conduction and the nature of electronic transport properties has been studied and discussed. It has been found that the complex perovskite oxides exhibiting high ionic conduction are located near the demarcation line separating localized and itinerant electrons. Such a characteristic can be understood in terms of the bond fluctuation model of superionic conductors. Our analysis has also revealed that

small difference in ionicity between A-O and B-O bonds is favorable for the ionic conduction.

References

[1] S.J. Skinner, Int. J. Inorg. Mater. 3 (2001) 113.

[2] K. Huang, J. Wan, J.B. Goodenough, J. Mater. Sci. 36 (2001) 1093.

[3] V.V. Kharton, F.M.B. Marques, A. Atkinson, Solid State Ionics 174 (2004) 135.

[4] T. Ishihara, Bull. Chem. Soc. Jpn. 79 (2006) 1155.

[5] S. Hashimoto, Y. Fukuda, M. Kuhn, K. Sato, K. Yashiro, J. Mizusaki, Solid State Ionics 186 (2011) 37.

[6] J.B. Goodenough, Rep. Prog. Phys. 67 (2004) 1915.

[7] K. Kamata, T. Nakamura, J. Phys. Soc. Jpn. 35 (1973) 1558.

[8] M. Aniya, Integr. Ferroelectr. 115 (2010) 81.

[9] R.D. Shannon, Acta Cryst. A 32 (1976) 751.

[10] J. Richter, P. Holtappels, U. Vogt, T. Graule, L.J. Gauckler, Solid State Ionics 177 (2006) 3105.

[11] H. Ullmann, N. Trofimenko, F. Tietz, D. Stöver, A. Ahmad-Khanlou, Solid State Ionics 138 (2000) 79.

[12] S. Taniguchi, M. Aniya, J. Phys. Soc. Jpn. 79 (Suppl. A) (2010) 106.

[13] P. Byszewski, R. Aleksiyko, M. Berkowski, J. Fink-Finowicki, R. Diduszko, W. Gebicki, J. Baran, K. Antonova, J. Mol. Struct. 792-793 (2006) 62.

[14] J.C. Phillips, Rev. Mod. Phys. 42 (1970) 317.

[15] H. Li, S. Zhang, S. Zhou, X. Gao, Mater. Chem. Phys. 114 (2009) 451.

[16] S. Taniguchi, M. Aniya, Integr. Ferroelectr. 115 (2010) 18.

[17] H. Hayashi, H. Inaba, M. Matsuyama, N.G. Lan, M. Dokiya, H. Tagawa, Solid State Ionics 122 (1999) 1.

[18] H. Ullmann, N. Trofimenko, J. Alloys Compd. 316 (2001) 153.

[19] M. Aniya, Solid State Ionics 50 (1992) 125.

[20] M. Aniya, F. Shimojo, Solid State Ionics 177 (2006) 1567.

[21] M. Aniya, K. Wakamura, Solid State Ionics 86-88 (1996) 183.

[22] L.J. Gauckler, D. Beckel, B.E. Buergler, E. Jud, U.P. Muecke, M. Prestat, J.L.M. Rupp, J. Richter, Chimia 58 (2004) 837.

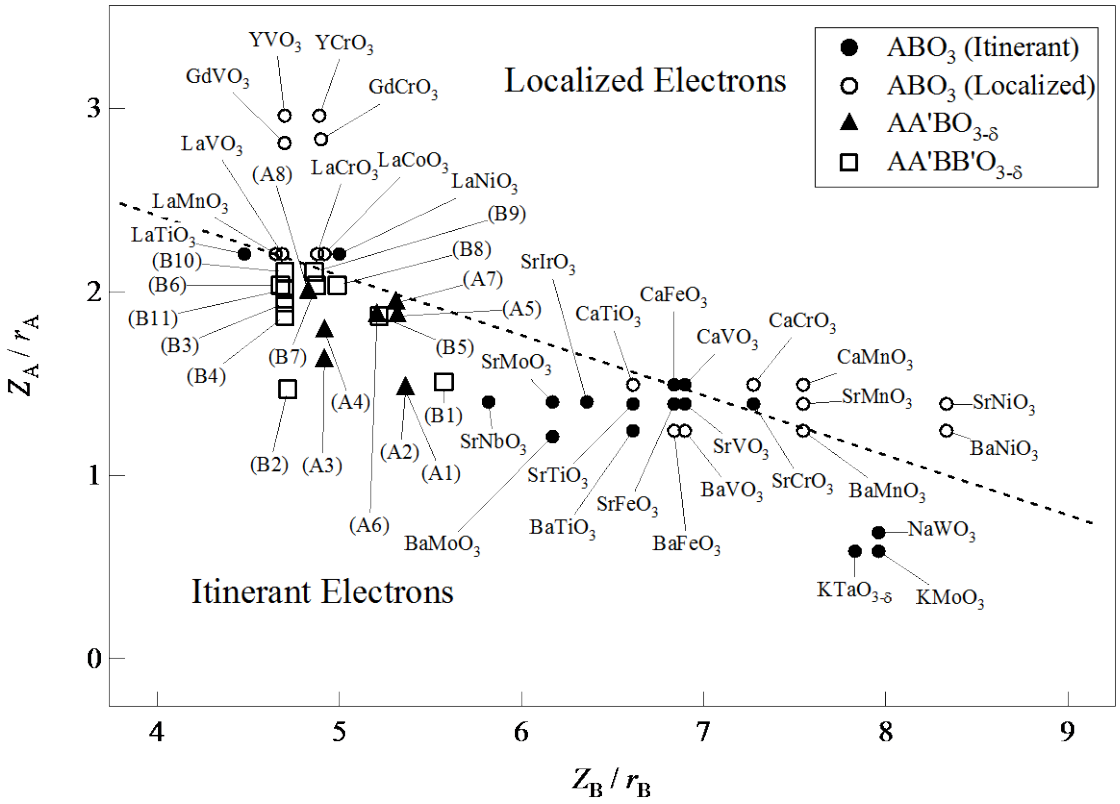

Fig. 1. Mapping of perovskite oxides in a space formed by Z_A / r_A and Z_B / r_B. The circle, triangle and square represent ABO_3, $A_{1-x}A'_xBO_{3-\delta}$ and $A_{1-x}A'_xB_{1-y}B'_yO_{3-\delta}$ compounds, respectively. The name of the compounds denoted by triangles and squares are given in Table 1.

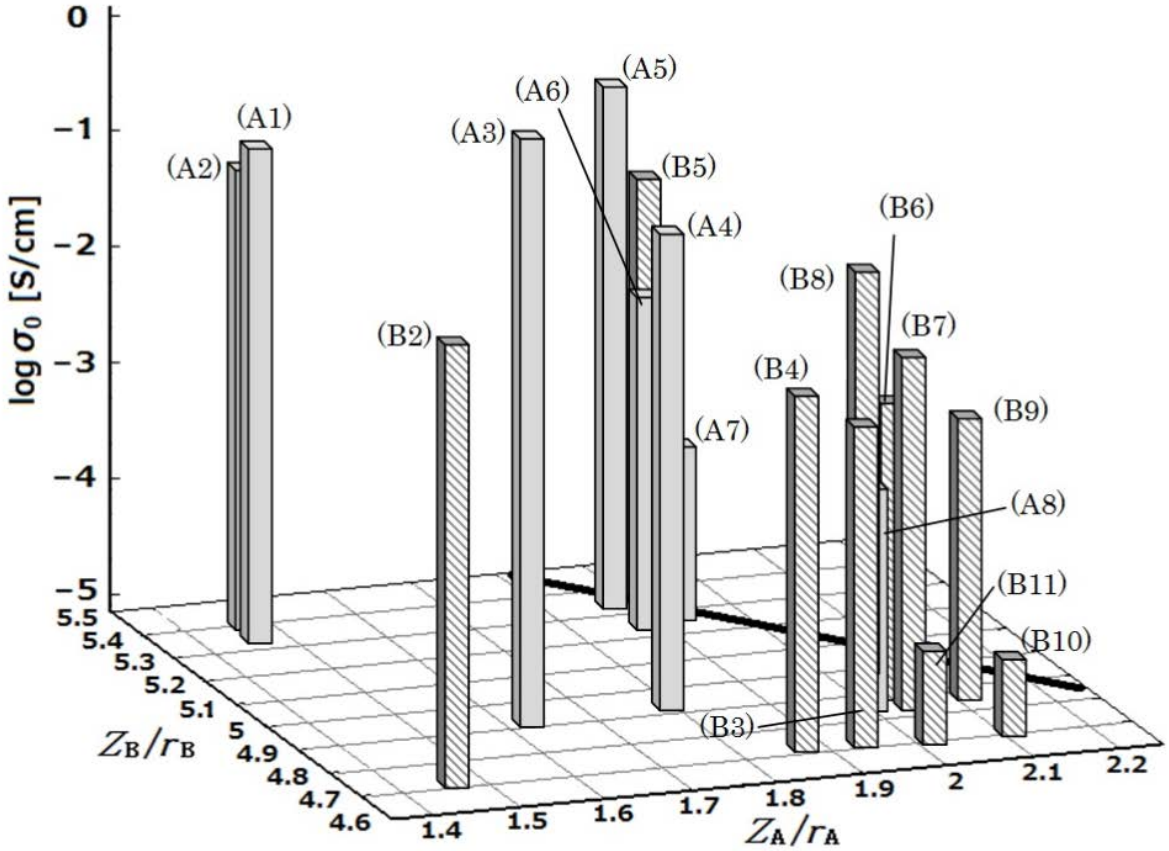

Fig. 2. A three-dimensional representation showing the relationship between the potential parameters of the cations and the oxygen ionic conductivity at T = 1073 K [11] in complex perovskite oxides. Gray and hatched vertical bars represent $A_{1-x}A'_xBO_{3-\delta}$ and $A_{1-x}A'_xB_{1-y}B'_yO_{3-\delta}$ compounds, respectively. The symbols denote the compounds given in Table 1. The full line in the basal plane is the demarcation line between localized and itinerant ABO_3 compounds shown in Fig. 1.

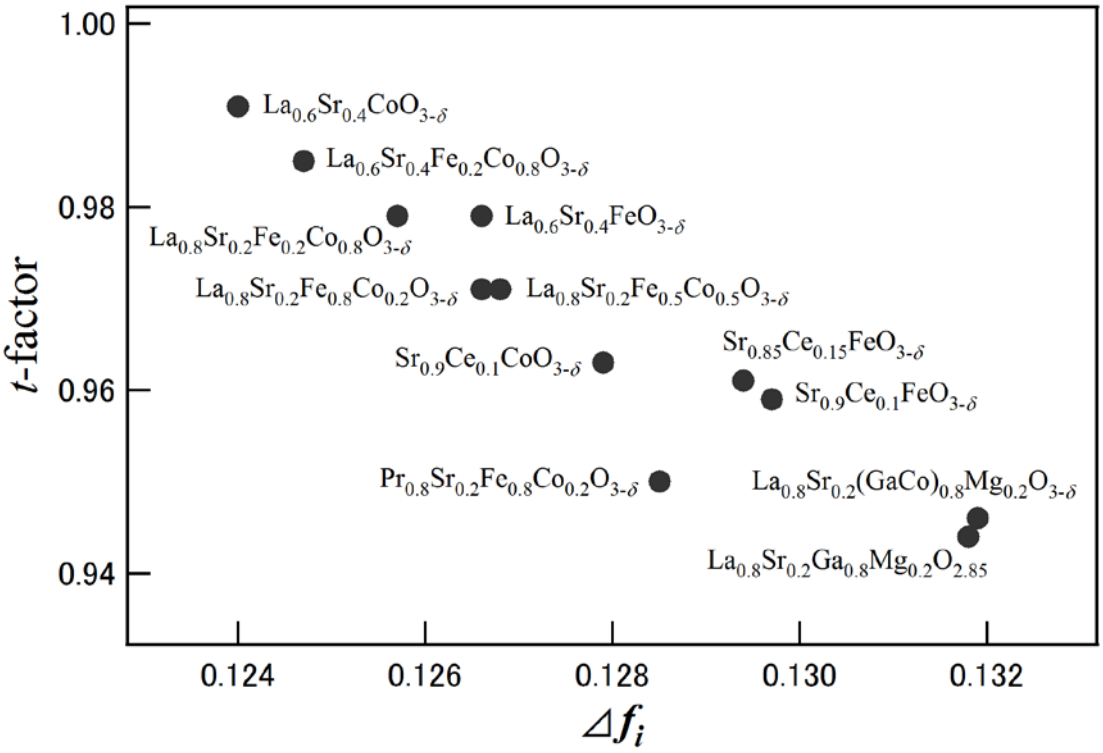

Fig. 3. Relationship between the difference of ionicity Δf_i and the tolerance factor in $A_{1-x}A'_xB_{1-y}B'_yO_{3-\delta}$ (A, A' = La, Ce, Pr, Sr / B, B' = Fe, Co, Mg, Ga) compounds.

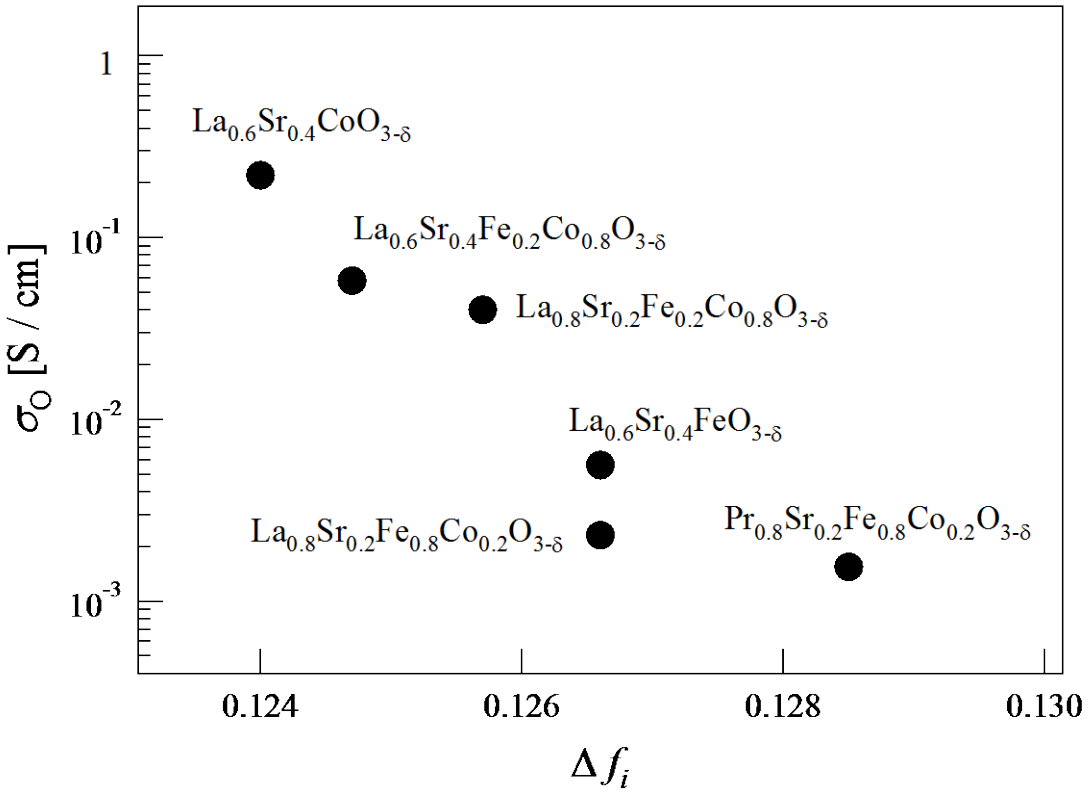

Fig. 4. Relationship between the oxygen ionic conductivity at T = 1073 K [11] and the difference of ionicity Δf_i in $A_{1-x}A'_xB_{1-y}B'_yO_{3-\delta}$ (A, A' = La, Pr, Sr / B, B' = Fe, Co) compounds.

Table 1. Compounds added into the map proposed in [7] and showed in Fig. 1. σ_0 are the values of the ionic conductivity at T = 1073 K reported in [11]. Values of the tolerance factors reported in [18] and Δf_i calculated through Eqs. (1) – (5) are also shown.

AA'BO$_{3-\delta}$		Z_A/r_A	Z_B/r_B	Δf_i	t-factor	σ_O [S/cm]
(A1)	$Sr_{0.9}Ce_{0.1}CoO_{3-\delta}$	1.469	5.361	0.1279	0.963	0.113
(A2)	$Sr_{0.9}Ce_{0.1}FeO_{3-\delta}$	1.469	5.364	0.1297	0.959	0.064
(A3)	$La_{0.3}Sr_{0.7}CoO_{3-\delta}$	1.624	4.918			0.76
(A4)	$La_{0.5}Sr_{0.5}CoO_{3-\delta}$	1.786	4.918			0.093
(A5)	$La_{0.6}Sr_{0.4}CoO_{3-\delta}$	1.868	5.318	0.1240	0.991	0.22
(A6)	$La_{0.6}Sr_{0.4}FeO_{3-\delta}$	1.868	5.206	0.1266	0.979	5.6×10^{-3}
(A7)	$La_{0.65}Sr_{0.3}MnO_{3-\delta}$	1.938	5.310		0.968	1.7×10^{-4}
(A8)	$Pr_{0.65}Sr_{0.3}MnO_{3-\delta}$	1.997	4.831		0.952	3.4×10^{-4}

AA'BB'O$_{3-\delta}$		Z_A/r_A	Z_B/r_B	Δf_i	t-factor	σ_O [S/cm]
(B1)	$Sr_{0.85}Ce_{0.15}Fe_{0.8}Co_{0.2}O_{3-\delta}$	1.509	5.574	0.1294	0.967	0.016
(B2)	$Sr_{0.9}Ce_{0.1}Fe_{0.8}Ni_{0.2}O_{3-\delta}$	1.469	4.717			0.04
(B3)	$La_{0.65}Sr_{0.3}Fe_{0.8}Co_{0.2}O_{3-\delta}$	1.938	4.702			4×10^{-3}
(B4)	$La_{0.6}Sr_{0.4}Fe_{0.8}Co_{0.2}O_{3-\delta}$	1.868	4.702			8×10^{-3}
(B5)	$La_{0.6}Sr_{0.4}Fe_{0.2}Co_{0.8}O_{3-\delta}$	1.868	5.219	0.1247	0.985	0.058
(B6)	$La_{0.8}Sr_{0.2}Fe_{0.9}Co_{0.1}O_{3-\delta}$	2.035	4.677			2.2×10^{-3}
(B7)	$La_{0.8}Sr_{0.2}Fe_{0.8}Co_{0.2}O_{3-\delta}$	2.035	4.875	0.1266	0.971	2.3×10^{-3}
(B8)	$La_{0.8}Sr_{0.2}Fe_{0.2}Co_{0.8}O_{3-\delta}$	2.035	4.989	0.1257	0.979	4×10^{-2}
(B9)	$Pr_{0.8}Sr_{0.2}Fe_{0.8}Co_{0.2}O_{3-\delta}$	2.108	4.862	0.1285	0.950	1.54×10^{-3}
(B10)	$Pr_{0.8}Sr_{0.2}Mn_{0.8}Co_{0.2}O_{3-\delta}$	2.108	4.702			3×10^{-5}
(B11)	$Pr_{0.7}Sr_{0.3}Mn_{0.8}Co_{0.2}O_{3-\delta}$	2.012	4.702			4.4×10^{-5}